PROCEEDINGS OF SCIENCE

The Impact and Status of the ILC Positron Source

G. Moortgat-Pick*
II. Inst. for Theoret. Physics, Hamburg University, Luruper Chaussee 149, D-22761 Hamburg,
Deutsches Elektronen Synchrotron (DESY), Notkestrasse 85, D-22607 Hamburg, Germany
E-mail: gudrid.moortgat-pick@desy.de

O. S. Adeyemi, A. Ushakov
II. Inst. for Theoret. Physics, Hamburg University, Luruper Chaussee 149, D-22761 Hamburg, Germany

F. Dietrich, S. Riemann
Deutsches Elektronen Synchrotron (DESY), Platanenallee 6, D-15738 Zeuthen, Germany

K. Flöttmann
Deutsches Elektronen Synchrotron (DESY), Notkestrasse 85, D-22607 Hamburg, Germany

High luminosity is required at future Linear Colliders which is particularly challenging for all corresponding positron sources. At the ILC, polarized positrons are foreseen, obtained from electron-positron pairs by converting high-energy photons produced by passing the high-energy main electron beam through a helical undulator. The conversion target undergoes cyclic stress with high peak values. To distribute the high thermal load, the target is rotated with 100 m/s. However, the cyclic stress over long time as well as the temperature dependent material parameters yield thermo-mechanical load which could exceed the recommended fatigue limit. In the talk, the impact of using the polarized positron source has been studied and a general overview about the ILC positron source components is given. XLThe target design parameters are reviewed, new results on the target stress evolution are shown as well as an outlook on approved prototype experiments is given.

The European Physical Society Conference on High Energy Physics
22–29 July 2015
Vienna, Austria

*Speaker.

PoS(EPS-HEP2015)519

1. The physics offer of the linear collider

The International Linear Collider (ILC) is a well designed e^+e^- linear collider with a foreseen c.m. energy range from $\sqrt{s} = 90-1000$ GeV. The Technical Design Report (TDR) [1] of this world-wide project has been finished in 2013. The project could be built close to the Kitakami site at Japan where currently very advanced engineering studies are ongoing towards a possible realization of such a project at the high-energy frontier.

The ILC offers high-precision physics at varaible energy scales and the currently foreseen energy stages are $\sqrt{s} = 250$ GeV ('Higgs boson frontier'), $\sqrt{s} = 350$ GeV ('Top quark threshold'), $\sqrt{s} = 500$ GeV ('Top-Yukawa coupling frontier'), $\sqrt{s} = 1000$ GeV ('Higgs potential'). If no new physics candidates appear at the LHC–, high luminosity run at $\sqrt{s} = 92$ GeV ('Electroweak physics precision frontier') is possible. A recent review of the physics potential of a linear collider is given in [2] .

A high luminosity of about $\mathscr{L} = 2\times 10^{34}$ cm^{-2}s^{-1} is envisaged as well as polarized initial beams. The ILC offers different experimental tools –such as tunable energy to allow for threshold scans as well as polarized initial beams[3] to access chirality– have an impact on the quantity as well as the quality of the experimental analyses and lead to a real 'add-on' compared to analyses at the Large Hadron Collider (LHC).

There have been discussed the expected physics outcome[4] of several running scenarios for dividing the luminosity at the different energy stages up to $\sqrt{s} \geq 500$ GeV based on a total running time of about 20 years [5]. The favourite scenario, called 'H20', foresees to collect in total 6200 fb^{-1} including the luminosity upgrade after 8 years of running time with the partition of 2000 fb^{-1} at $\sqrt{s} = 250$ GeV, 200 fb^{-1} at $\sqrt{s} = 350$ GeV and 4000 fb^{-1} at $\sqrt{s} = 500$ GeV.

The high luminosity demands are in particular challenging for the positron source at linear colliders. The foreseen undulator-based e^+ source at the ILC has been chosen as the most mature design for coping with the luminosity demands and offers in addition simultaneously polarized positrons. In [5] it is also discussed how to divide up the luminosity between the four different polarization configurations $(-,+)$, $(+,-)$, $(+,+)$, $(-,-)$ (where the first(second) argument denotes the e^- (e^+) helicity). Switching both helicities on a regular basis is unavoidable in order to get systematics and correlations between $P_- \times P_+$ under control (see contribution of L. Malysheva in[6]) and to enhance the actual number of interactions.

Before we describe the technical status of this polarized e^+ source and address in particular the target issues in details, we compare shortly the current physics expectations with the case if only an unpolarized positron source was used.

1.1 Impact of positron polarization

Physics processes occur through e^-e^+–annihilation ('s'–channel diagrams) and –scattering ('t,u'–channel diagrams). In annihilation diagrams the helicities of the incoming beams are coupled to each other, whereas in scattering processes, they are coupled to the produced particles and therefore are directly sensitive to their chiral properties. Only in such processes $P(e^+)$ can uniquely test the couplings of the produced 'new' particles.

Both Higgs physics as well as precision top quark physics strongly benefits from the use of polarized beams. Furthermore new physics will manifest itself with new fermionic and bosonic particles carrying unknown chiral couplings and spins. Disentangling and studying the underlying physics strongly benefits from the polarization of both beams because in that case a higher effective degree of polarization, a reduced uncertainty of the polarisation measurement and an efficient suppression of background processes with suitably polarized states is achievable. In addition simultaneously polarized positron beams offer a higher number of observables and allow to extract new characteristics of interactions. These are unique features that cannot be compensated by just offering a higher polarization of only the electron beam.

- The polarisation will be increased effectively to a value $P_{eff} = (P_- + P_+)/(1 + P_- P_+)$: for example, 80% electron and 60% (30%) positron polarisation result in an effective polarization of 95% (88%). The number of interactions can be enhanced since the effective luminosity is given by $\mathscr{L}_{\text{eff}}/\mathscr{L} = 1 - P - e^- P_{e^+}$ and will be increased by a factor 1.48 (1.24) in such cases.
- Due to error propagation the polarisation uncertainty is substantially reduced if the positrons are polarized simultaneously: For the configuration $(|P_{e^-}|, |P_{e^+}|) = (80\%, 60\%)$ and (80%, 30%), the uncertainty of the effective polarisation is smaller by factor 4 and 2, respectively, for independent polarization errors ΔP_-, ΔP_+ and at least by a factor of 3 and 1.5, correspondingly, for correlated errors, compared with only $(80\%, 0\%)$.
- The cross sections can be enhanced or reduced by an appropriate choice of the polarization states. This allows to reduce the background by suppressing undesired polarization states: The ratio of 'wrong' to 'right' polarization states in many processes is $[(1 + P_-)(1 - P_+)]/[(1 - P_-)(1 + P_+)]$ and yields a background reduction by a factor of 4 (2) having (80%,60%) ((80%,30%)) polarization instead of (80%,0). A positron polarisation of 30% reduces therefore already the undesired background by a factor 2 compared to only polarized electrons.

If both beams are polarized another experimental option is available: the use of transversely polarized beams, (if only one beam is polarized in the Standard Model and most Beyond Standard Models all effects at leading order from transverse polarization vanish for $m_e \ll \sqrt{s}$). Transversely polarized beams are, for instance, advantageous for the direct study of CP-violating asymmetries in new physics models and for model distinction in indirect searches for extra dimensions and are required to access CP-violating triple gauge couplings.

In the following we concentrate only on the physics gain of polarized beams in the Higgs and top quark physics sector. More details as well as a comprehensive discussion of the impact of polarized beams in physics topics beyond the Standard Model as well as in high precision studies at the Z-pole or WW-threshold, see [3] and references therein.

1.2 Higgs sector

The discovery of a Higgs boson in 2012 offered many new urgent physics questions: is it really the only Higgs boson of the Standard Model or one of the supersymmetric Higgs bosons or is even a composite state? In order to manifest whether the Higgs boson is really the Higgs boson predicted within the Standard Model, couplings and branching ratios have to be measured

PoS(EPS-HEP2015)519

very precisely. Precision within the 1%–2% is required, see Fig. 1, to be sensitive to non-SM couplings. A crucial input for all couplings fit is the cross section of the Higgs-strahlung, as can be seen in Fig. 2 (left panel): here, the achievable precision in the different Higgs couplings at the LHC on bases of 3 $\text{ab}^{-}1$ and 50% improvement in the theoretical uncertainties in comparison with the different energy stages at the ILC [7] has been studied. However, since the polarized cross section is given by the scaling factor $\sigma_{\text{pol}}/\sigma_{\text{unpol}} \sim (1-0.151 P_{\text{eff}}) * \mathscr{L}_{\text{eff}}/\mathscr{L}$, one loses about 30% in the cross section if no positron polarization were provided. The dominant background is ZZ (for leptonic final state) and WW (for hadronic final state), so that one would lose in the significance $S/\sqrt{B}$ for this process about 20% (for leptonic final state) and even about a factor 2 (for hadronic final state) if no polarized positrons were available.

Another crucial but very challenging coupling for both collider experiments, LHC and ILC, is the trilinear Higgs coupling, characteristic for the Higgs potential and the mechanism of electroweak symmetry breaking. The cross sections at the LC are far below 1 fb for $\sqrt{s} < 1$ TeV. Both channels, Higgs-strahlung as well as WW-fusion, are required as can be seen from Fig.2 (right panel). With the full physics programme up to $\sqrt{s} = 500$ GeV, currently a precision of $\delta\lambda/\lambda \sim 27\%$ seems to be achievable at the ILC. If no positron polarization were available these expectations could not be matched within the given luminosity. After an upgrade to $\sqrt{s} = 1$ TeV a precision of about 10% or better will be achievable[8].

No official number for the expected preision can currently be given at the LHC.

1.3 Top sector

In the top-quark sector, in particular, two urgent topics arises: the determination of the electroweak top-quark couplings in general and of the top-quark Yukawa-coupling. These measurements are important to open a possible window for new physics contributions. In particular the latter is very promising and its precise determination is crucial. Is has been shown by [8, 4] that a precision of $\sim 6.3\%$ would be achievable at $\sqrt{s} = 500$ GeV (incl. luminosity upgrade). A further increase of the energy of about 10% might be very promising as well, allowing a precision of about 3% at $\sqrt{s} = 550$ GeV instead of 6.3% at $\sqrt{s} = 500$ GeV. However, if no polarized positrons might be available a decrease of about 20% is expected. Contrary, if even $P_{e^+} = 60\%$ were available instead of only 30% a further increase of about 25% is provided, cf. Fig. 3 (left panel).

The determination of the top-quark electroweak couplings is challenging at the LHC, Fig. 3 (right panel). However, with the help of different possible observables, cross sections and angles, these couplings are accessible at the ILC up to the %–level [9, 10]. The positron polarization is mandatory in this regard in order to allow model-independent fits and plays a crucial role to enable the expected precision.

2. The ILC positron source: overview

From the listed physics requirements and expected running scenarios, it is obvious that the positron source is a challenging component at any LC. In the ILC baseline design an undulator-based positron source has been chosen as the mature design, coping with the high luminosity requirements. The energy of the electron drive been is foreseen in the range of 120 GeV –250 GeV, even at 500 GeV for the energy upgrade option, see Fig.4 (left panel). The undulator parameters are chosen so that a yield of 1.5 e^+/e^-, i.e. a safety margin of 50%, is fulfilled. A damping ring acceptance of $\varepsilon_{nx} + \varepsilon_{ny} \leq 70$ mm rad has to be achieved. Since a helical undulator is used —because of the higher yield compared to a planar undulator— the positron source is polarized and provides a polarization degree of about 30% with the given parameters (see below) and can be upgraded to 60% with the help of a collimator. A more detailed sketch is layed out in Fig. 4(right panel): the undulator is foreseen with a maximal length of 231 m, a period of 11.5 mm and a K value of 0.92. For the polarization upgrade a photon collimator has already been designed [11]. The target is Ti-Alloy of 0.4 radiation length and rotates with a tangential speed of 100 m/s. The optical matching device is a flux concentrator in combination with a 10 m length normal conducting capture RF system. For a drive-beam of 120 GeV the full length of 231 m is required. Using in a addition a collimator with $r = 3.5$ mm would lead to $P_{e^+} = 40\%$. Already at the top-quark threshold, $\sqrt{s} = 350$ GeV the polarization could be increased up to 56% adjusting the collimator to $r = 1.2$ mm. At the design energy $\sqrt{s} = 500$ GeV only a length of 144 m is required, providing even $P_{e^+} \sim 60\%$ for $r = 0.7$ mm. At the upgrade energy of $\sqrt{s} = 1$ TeV, the undulator parameter have to be adjusted to achieve a reasonable polarization of about $P_{e^+} = 54\%$, if a K-value of 2.5, an undulator length of 176 m and the collimator radius of $r = 0.9$mm have been chosen (more details, see contribution of A. Ushakov in [6]).

Te baseline source parameter are listed in Fig. 5. One has to note that the photon energy is about 43 MeV if the undulator field is $h = 0.42$, however, if one increases the field to $h = 0.92$ the photon energy of the 1st harmonic is reduced to 30 MeV. With FLUKA detailed simulations have been performed to study the energy deposition in the target. In Fig. 6, one sees the distribution of the energy density distributed by one bunch. The target length is 1.48 cm. The beam goes in z-direction, the target is radial oriented with a radius of 1.5 cm in xy-direction. The corresponding energy profile of the peak energy deposition (per bunch) are depicted in Fig. 7 in transverse (left panel) and longitudinal direction (right panel), see also [12] for an analytical approach. A very important parameter concerning the thermal target stress is the temperature rise and distribution, that has been simulated with ANSYS, see Fig. 8. The time between two bunches is about 550 ns.

As next step the temperature distribution in a rotated target after one pulse length has been simulated. The rotation velocity is 100m/s at the rim of the target. A full pulse length contains 1312 bunches and takes 0.727 ms. Therefore the total absorbed energy is 43 kW$\times$5.3% per 5 Hz=456 J, cf. Fig. 5. This results in a average power per pulse of 627 kW and a peak power density distribution in the target volume of 276 kW/cm^3. The corresponding peak density distribution density (PEDD) per pulse is of about 45 J/g, see Fig. 9. A peak corresponds to 100 bunches, hitting one single point at the target. In Fig. 10 (left panel) the normal stress components $s_1 + s_2 + s_3$ have been simulated (the shear stress components have been neglected since they are expected to be one order of magnitude smaller). The sum of the normal stress after one full pulse within this model would lead to a maximum pressure of about 176 MPa. This result has been compared with results corresponding to the approximation of van Mises stress. Within such a model, where the shear stress components are included in an approximation, one reaches the maximum of 108 MPa after one complete pulse. Just for comparison, for Titanium the maximum peak value in the literature is 820 MPa and a continuums value of about 340 MPa seems to be acceptable. One has to note, however, that the dynamical effects and Eddy currents are not yet included, but seem to be at an acceptable level.

3. Planned experiments

There exist a strong demand for a reliable value of the corresponding material fatigue limit. It is therefore planned to use an high intensity electron beam with high currents and reduce the beam size and thickness until dE/dV is comparable to the target conditions at the ILC. The thermal stress is mimicked via long ($\sim 20\ \mu$s) electron pulses. Different target materials and in different geometries will be tested. Such an experiment is already approved at MAMI and at the future MESA experiment at Mainz. A the currently running MAMI accelerator one has an injector with 1 mA at 3.5 MeV. It is foreseen to use the beam spot target-thickness scale of 1/10 mm, reducible up to 10 μm. Due to the c.w. capability a high repetition rate is achievable so that an 'artificial aging' effect will be obtained.The experiment starts in fall 2015. At the MESA experiment the preaccelerator runs at 5-8 MeV but with 10 mA at 5-14 MeV. This experiment is planned to start in 2017. Definitely at the latter experiments comparable target stress as at the ILC will be achieved so that a reliable fatigue limit of the target is obtained.

4. Conclusions

As concluding remark one can state that the baseline ILC positron source is well designed and at a mature level, providing high luminosity and high polarization for all different energy stages.. However still target issues, that are relevant for all LC design, arises. Therefore bunch-by-bunch simulations of thermal stress that are induced by the photon beam have been performed. The current simulations (still ongoing) show that the fatigue limit will not be reached by far. However, real target geometries and sound wave reflections have still to be included. Backup simulations with analytical calculations and different models have been performed as well.

A two-stages experiment at Mainz has ben approved where the fatigue limit of different target materials and geometries will be tested. At the MAMI and later at the MESA accelerator comparable energy densities as at the ILC can be achieved at the target via artificial aging. The results will provide reliable limits of the fatigue limits in an radiation environment comparable with the conditions at the ILC.

G.M-P. would like to thank the organiser of the EPS conference at Vienna for a very welcoming, very pleasant and just perfect organization . Thhe work is supported by the German Federal Ministry of Education and research, Joint Research Project R&D Accelerator "Positron Sources", contract number 05H2015.

References

[1] T. Behnke *et al.*, arXiv:1306.6327 [physics.acc-ph]; H. Baer *et al.*, arXiv:1306.6352 [hep-ph]; C. Adolphsen *et al.*, arXiv:1306.6353 [physics.acc-ph]; C. Adolphsen *et al.*, arXiv:1306.6328 [physics.acc-ph]; T. Behnke *et al.*, arXiv:1306.6329 [physics.ins-det].

[2] G. Moortgat-Pick *et al.*, Eur. Phys. J. C **75** (2015) 8, 371 [arXiv:1504.01726 [hep-ph]].

[3] G. Moortgat-Pick *et al.*, Phys. Rept. **460** (2008) 131 [hep-ph/0507011].

[4] K. Fujii *et al.*, arXiv:1506.05992 [hep-ex].

[5] T. Barklow, J. Brau, K. Fujii, J. Gao, J. List, N. Walker and K. Yokoya, arXiv:1506.07830 [hep-ex].

[6] G. Moortgat-Pick *et al.*, "Helmholtz Alliance Linear Collider Forum : Proceedings of the Workshops Hamburg, Munich, Hamburg 2010-2012, Germany," doi:10.3204/DESY-12-123H

[7] P. Bechtle, S. Heinemeyer, O. St?l, T. Stefaniak and G. Weiglein, JHEP **1411** (2014) 039 doi:10.1007/JHEP11(2014)039 [arXiv:1403.1582 [hep-ph]].

[8] C. Dürig, talk given at this conference, Vienna, 2015.

[9] M. S. Amjad, T. Frisson, E. Kou, R. Poschl, F. Richard and J. Rouene, Nuovo Cim. C **037** (2014) 02, 55; M. S. Amjad et al., arXiv:1505.06020 [hep-ex].

[10] A. Juste et al., ?Report of the 2005 Snowmass Top/QCD Work- ing Group?, econf/C0508141:PLEN0043 (2005), arXiv:hep- ph/0601112.

[11] S. Riemann, F. Staufenbiel, G. Moortgat-Pick and A. Ushakov, *"Photon collimator system for the ILC Positron Source,"* arXiv:1412.2498 [physics.acc-ph].

[12] Olufemi Segun Adeyemi, *"Linear Acoustic Waves Induced in a Cylindrical Solid Target by Particle Beam in $e^- - e^+$ Colliders,"* DESY-THESIS-2015-020, PhD Thesis University of Hamburg, 2015.

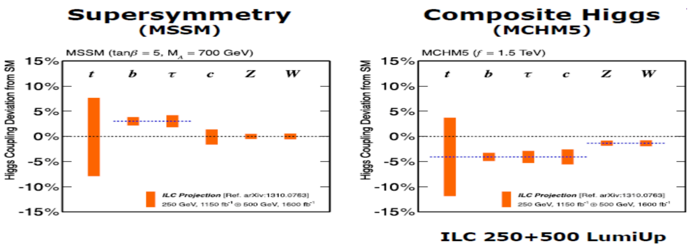

Figure 1: Comparison of Higgs boson couplings within Supersymmetry (MSSM) and a composite Higgs model (MCHM5) compared to the Standard Model. As can be seen from the figure, an experimental accuracy of 1-2% will be required to be sensitive to non-Standard Model couplings.

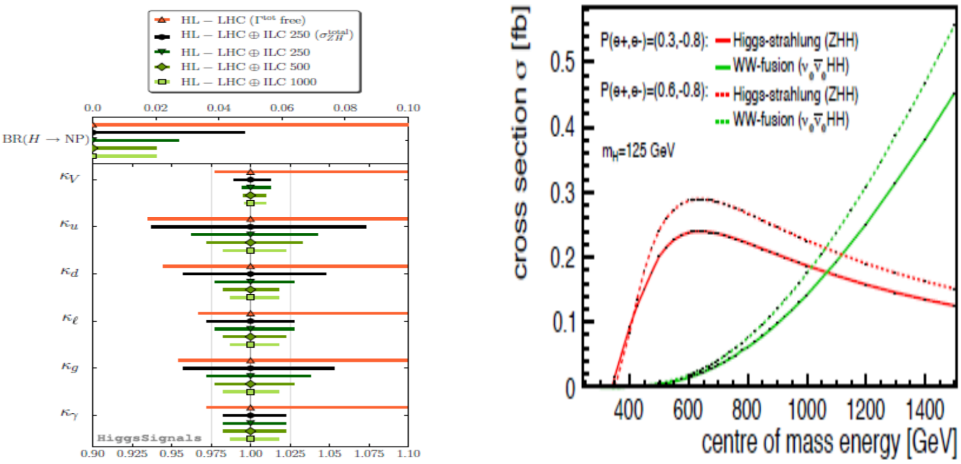

Figure 2: Left: The achievable precision in the different Higgs couplings at the LHC on bases of 3 ab^{-}1 and 50% improvement in the theoretical uncertainties in comparison with the diferent energy stages at the ILC[7]. Right: Cross section for the double Higgs production processes, $e^+e^- \to Zhh$ and $e^+e^- \to \nu\bar{\nu}hh$, as a function of $\sqrt{s}$.

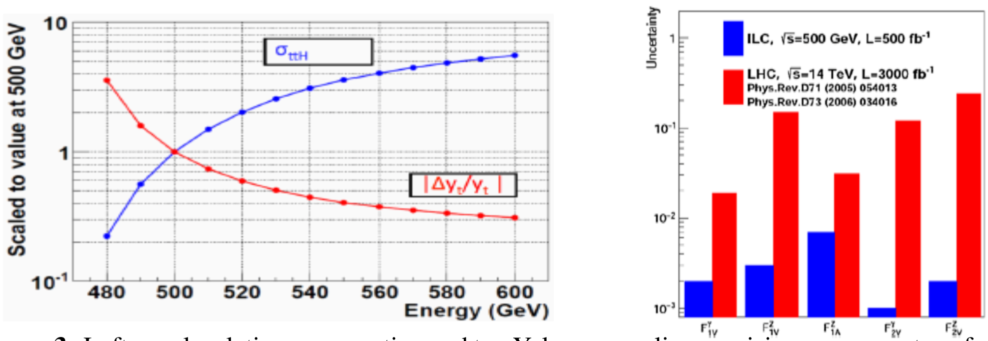

Figure 3: Left panel: relative cross section and top Yukawa coupling precision versus centre-of-mass energy, extrapolated based on scaling of signal and main background cross-sections [5]. Right panel: Statistical precision on CP-conserving form factors expected at the LHC [10] and at the ILC [9]. The LHC results assume an integrated luminosity of $\mathscr{L} = 300\ \mathrm{fb}^{?1}$. The results for the ILC are based on an integrated luminosity of $\mathscr{L} = 500\ \mathrm{fb}^{?1}$ at $\sqrt{s} = 500$ GeV and a beampolarization of $P_{e^?} = \pm 80\%$, $P_{e^+} = \mp 30\%$ [9].

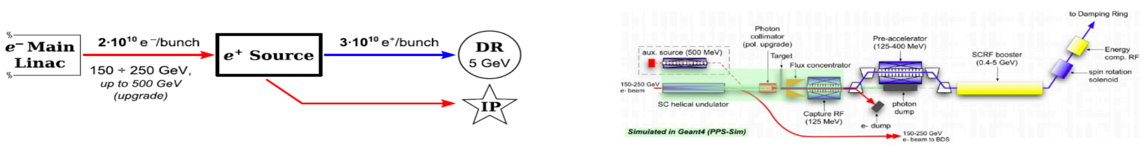

Figure 4: Left panel: ILC positron source requirements. Right panel: Schematic layout.

e^- Energy [GeV]	250
Number e^- per Bunch	$2 \cdot 10^{10}$
Number of Bunches per Pulse	1312
Bunch Spacing [ns]	554
Pulse Repetition Rate [Hz]	5
Undulator Field [T]	0.42
Photon Energy (1st harmonic) [MeV]	42.9
Required Undulator Length [m]	147
Average Photon Power [kW]	43
Relative Energy Deposition in Target [%]	5.3
Photon rms spot size on target [mm]	0.8

Figure 5: Parameters of the e^+ source of the ILC baseline design.

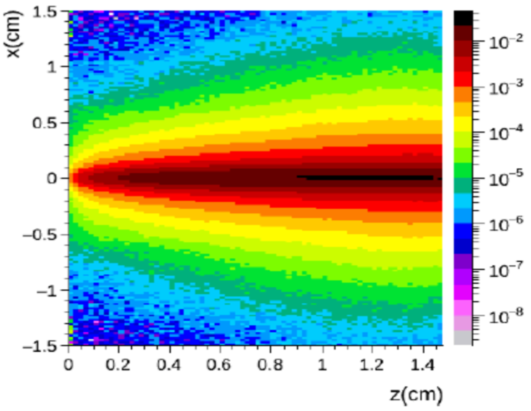

Figure 6: Energy deposition inside the ILC baseline target, simulated with FLUKA.

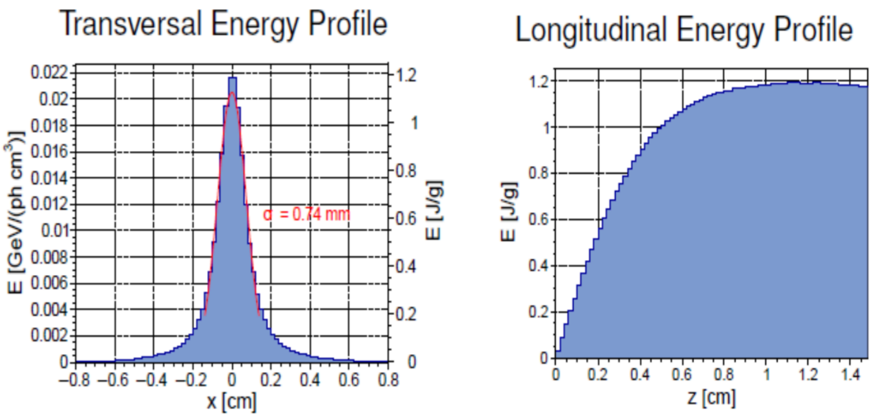

Figure 7: Peak energy deposition per bunch in transversal direction (left panel) and in longitudinal direction (right panel).

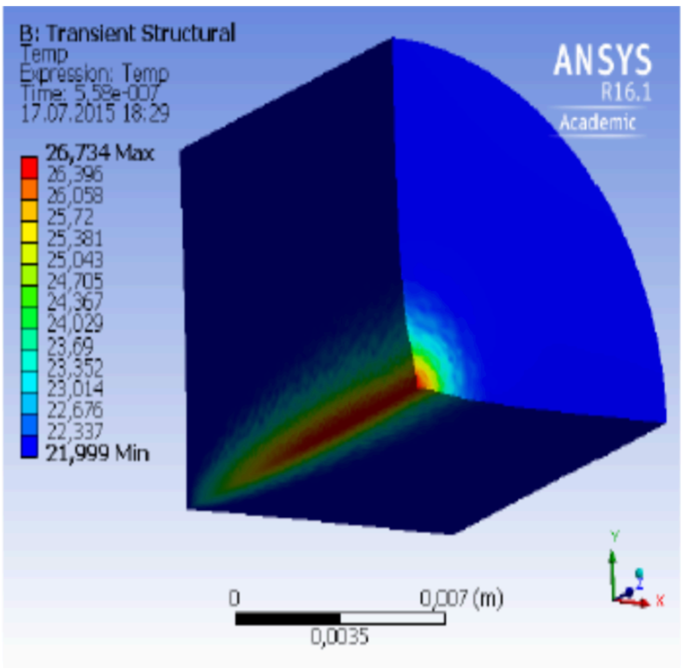

Figure 8: The temperature rise and distribution inside the ILC target, simulated with ANSYS.

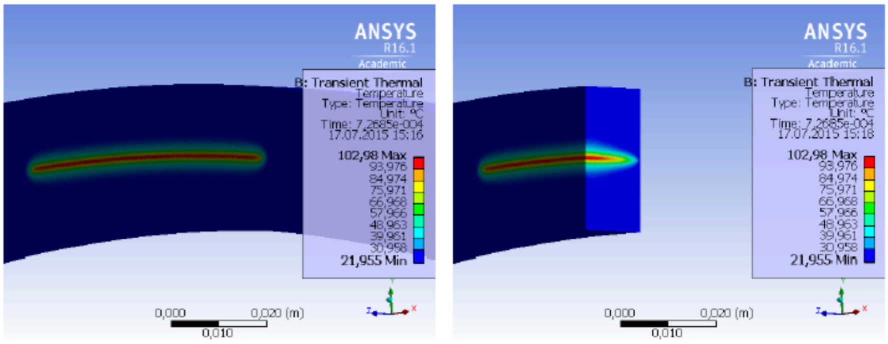

Figure 9: Temparature distribution in the rotated target (100 m/s at the rim) after the 1st pulse..

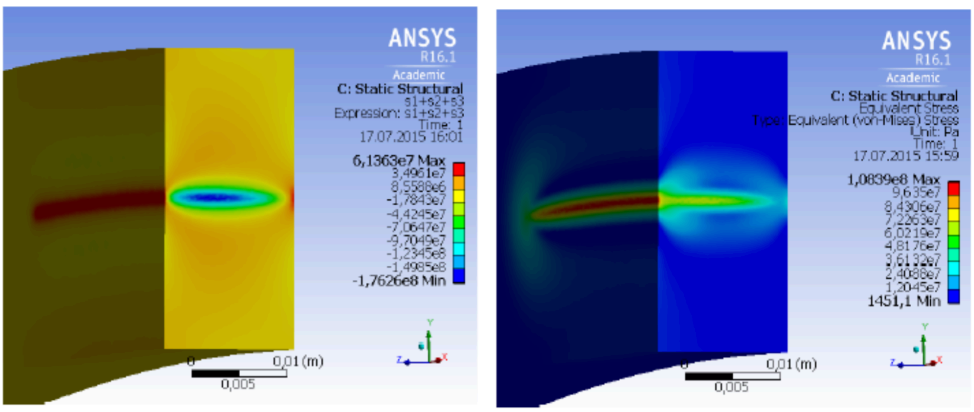

Figure 10: The complete sum of normal stress components leading to 176 MPa compared with the approximation of von Mises stress where shear stresses are included.